Mass Transport Investigated with the Electrochemical and Electrogravimetric Impedance Techniques. 2. Anion and Water Transport in PMPy and PPy Films

Haesik Yang and Juhyoun Kwak*

Department of Chemistry, Korea Advanced Institute of Science and Technology, Taejon 305-701, Korea

Received: March 12, 1997[⊗]

Water transport during anion transport in poly(*N*-methylpyrrole/nitrate) (PMPy/NO_3), poly(*N*-methylpyrrole/chloride) (PMPy/Cl), and poly(*N*-methylpyrrole/sulfate) (PMPy/SO_4) films, where ion transport is anion-specific, has been investigated by comparing electrical responses with gravimetric responses in the cyclic electrochemical quartz crystal microbalance (EQCM) experiment and the impedance experiment. It is shown that the number of accompanying waters per Cl^- or SO_4^{2-} is considerable, whereas the number per NO_3^- is not large. The number of accompanying waters per anion does not change extensively with the concentration of an electrolyte solution and the applied potential. Moreover, the possibilities of OH^-, H^+, cation, and water transport in poly(pyrrole/nitrate) (PPy/NO_3) and poly(pyrrole/chloride) (PPy/Cl) films, where ion transport is not anion-specific, have also been investigated. It is found that OH^- moves competitively with NO_3^- or Cl^- during their redox reaction.

Introduction

The redox reaction of a conducting polymer film is accompanied by ion transport into or out of the film. Because the ion transport behavior governs its redox properties, many efforts have been directed to the studies on the ion transport mechanism.[1]

Recently, we have obtained important information on cation and accompanying waters[2] during the redox reaction of poly(pyrrole/copper phthalocyaninetetrasulfonate) (PPy/CuPTS) films[3] by use of the electrochemical quartz crystal microbalance (EQCM) technique,[4] the electrochemical impedance technique,[5] and the electrogravimetric impedance technique.[6] The number of accompanying waters per cation depends on the hydration number of a cation in an electrolyte solution; it increases with the sequence of $Cs^+ < K^+ < Na^+ < Li^+ < Mg^{2+}$ and increases as the electrolyte concentration decreases. The number of accompanying waters per cation exhibits the hysteresis behavior during the redox cycle and increases during insertion of a cation whereas it is uniform during exclusion of a cation.

The dominant ionic species depends on the choice of the dopant anion and the solvent/electrolyte system.[7] It has been known that anion transport is dominant in the film doped with a small-size anion such as poly(pyrrole/nitrate) (PPy/NO_3) films,[8] poly(pyrrole/chloride) (PPy/Cl) films,[9] and poly(pyrrole/perchlorate) (PPy/ClO_4) films.[10] It was reported that the contribution of a cation is small in the aqueous solution where the cation is composed of only a divalent cation such as Ba^{2+}.[11] It was also reported that the mass change during the redox reaction of PPy/Cl films does not show Cl^--permselective behavior,[9] that H^+ is involved in ion transport during the redox reaction of PPy/Cl films,[9] and that OH^- transport is considerable during the redox reaction of PPy/NO_3 films.[8b,c] Moreover, when the mass change is less than that in ion-specific transport, the small mass change has been explained by counterion transport[3,8a,7b,9] or counter-directional water transport.[3,12] Thus, there is the possibility of OH^-, H^+, cation, or water transport in addition to anion transport in the PPy films.

There have been many studies on anion and water transport in redox polymer films such as poly(vinylferrocene) films[13] and $[Os(bpy)_2(PVP)Cl]^+$ films,[14] where the number of accompanying waters per anion is very large. On the other hand, in conducting polymer films, there is no quantitative data for the number of accompanying waters per anion, although much of the work has been focused on the anion transport mechanism. In this study, anion and water transport for poly(*N*-methylpyrrole) (PMPy)[15] and PPy films in aqueous electrolyte solutions have been investigated from both cyclic EQCM experiment and impedance experiment. Electrical responses (current or electrochemical capacitance) and gravimetric responses (mass change rate or electrogravimetric capacitance) have been compared to clarify the anion and water transport behavior. First, the number of accompanying waters per anion for poly(*N*-methylpyrrole/nitrate) (PMPy/NO_3), poly(*N*-methylpyrrole/chloride) (PMPy/Cl), and poly(*N*-methylpyrrole/sulfate) (PMPy/SO_4) films in electrolyte solutions containing a divalent cation is investigated in terms of the nature of an electrolyte solution and their redox state. And then, in PPy/NO_3 and PPy/Cl films, the possibilities of cation, water, OH^-, and H^+ transport in addition to NO_3^- and Cl^- transport, respectively, are examined.

Experimental Section

Chemicals. *N*-Methylpyrrole, pyrrole, $NaNO_3$, $Mg(NO_3)_2$, $Ca(NO_3)_2$, $Ba(NO_3)_2$, $MgCl_2$, $BaCl_2$, $MgSO_4$, and D_2O were purchased from Aldrich and used as received. Double-distilled water was used for the preparation of all solutions.

Electrochemistry and Film Preparation. An electrochemical cell and electrodes used in this study were the same as those reported previously.[2] PMPy/NO_3 films were grown potentiostatically at 0.65 V vs Ag/AgCl in a solution of 0.05 M *N*-methylpyrrole and 0.2 M $NaNO_3$. Because the thickness of PMPy/Cl and PMPy/SO_4 films grown in Cl^-- and SO_4^{2-}-containing solutions, respectively, is not uniform, it is difficult to obtain the exact mass change in the gravimetric experiment. Therefore, PMPy/Cl and PMPy/SO_4 films were obtained from several redox cycles of PMPy/NO_3 films in Cl^-- and SO_4^{2-}-containing solutions, respectively. The mass change and current behaviors during the redox cycle for the ion-exchanged PMPy/Cl and PMPy/SO_4 films were similar to those for the PMPy/Cl and PMPy/SO_4 films polymerized in Cl^-- and SO_4^{2-}-containing solutions. The charge consumed during the polymerization of

* Author to whom correspondence should be addressed.

S1089-5647(97)00924-3 CCC: $14.00

PMPy films is 300 mC/cm^2. PPy/NO_3 and PPy/Cl films were grown at 0.55 V in a solution of 0.1 M pyrrole and 1 M $NaNO_3$ and in a solution of 0.1 M pyrrole and 1 M NaCl, respectively. The film thickness of PPy films is estimated by assuming that 300 mC/cm^2 corresponds approximately to 1 μm with consideration of the reported value.[16] Unless stated otherwise, the film thickness of PPy films is 1 μm. After the polymerization, the cell and the film were washed with distilled water, and then fresh electrolyte was introduced into the cell. All cyclic data in the cyclic EQCM experiment were measured during the second cycle of two consecutive cycles after being held at the positive potential limit.

The experimental apparatus and the data treatment were described previously.[2] It was shown that the comparison of the mass change obtained from the electrochemical impedance of a quartz crystal with the mass change from the resonance frequency of an oscillating quartz crystal verifies the linear relation between resonant frequency and mass.[2,17] In this experiment, there is no significant difference between the mass change from the electromechanical impedance and the mass change from the resonant frequency. Thus, the mass change in the gravimetric experiment was obtained from the resonant frequency without consideration of the morphology change of the film. The calibrated mass sensitivity is 4.42 ng/Hz.

Results and Discussion

Water Transport in PMPy/NO_3, PMPy/Cl, and PMPy/SO_4 Films. Figure 1 shows cyclic voltammograms and simultaneously acquired mass change diagrams for PMPy/NO_3, PMPy/Cl, and PMPy/SO_4 films in aqueous electrolyte solutions. To compare mass charge rate ($G = dM/dt$) with current (I), G can be normalized by the factor $-(zF/W')$, i.e.,

$$G_n = -(zF/W')G \quad (1)$$

where G_n is normalized mass change rate, z is the electric charge of an ion, and F is the Faraday constant. If the mass change of a film is caused by the movement of only one kind of ion and accompanying waters, W' is given by

$$W' = W + YW_s \quad (2)$$

where W is the molar mass of an ion, Y is the number of accompanying waters per ion, and W_s is the molar mass of water. In all mass change rate diagrams, G is normalized without consideration of water transport ($W' = W_{NO_3^-}$, $W' = W_{Cl^-}$, and $W' = W_{SO_4^{2-}}$).

During the redox reaction of a PMPy/NO_3 film in a 0.1 M $Mg(NO_3)_2$ solution (Figure 1a), G_n is similar to I in an overall potential range. In a 0.1 M $Ba(NO_3)_2$ solution (Figure 1b), G_n also shows similar behavior with I. Moreover, I and G_n in Figure 1b are similar to those in Figure 1a. If cation movement in the opposite direction of NO_3^- movement was considerable, G_n would be much smaller than I, and G_n in a Ba^{2+}-containing solution would be smaller than that in a Mg^{2+}-containing solution because the molar mass of Ba^{2+} ($W_{Ba^{2+}} = 137.3$) is much larger than $W_{Mg^{2+}}$ (=24.3). It is evident that cation transport is negligible in this system. If anion-specific transport was accompanied by considerable water transport at any potential, G_n would be much larger than I. It is also evident that water transport is not large during NO_3^- transport.

During the redox reaction of a PMPy/Cl film in a 1 M $Mg(Cl)_2$ solution (Figure 1c), G_n is larger than I in a overall potential range. In a 1 M $Ba(Cl)_2$ solution (Figure 1d), G_n is also larger than I. Noting that I and G_n in a 1 M $Mg(Cl)_2$ solution are similar to those in a 1 M $Ba(Cl)_2$ solution, it is clear that cation transport is also not important during Cl^- transport. Therefore, it can be concluded that the discrepancy between G_n and I is caused by the considerable number of accompanying waters per Cl^- (Y_{Cl^-}). During the redox reaction of a PMPy/SO_4 film in a 1 M $MgSO_4$ solution (Figure 1f), G_n is also larger than I in most potential range, indicating that $Y_{SO_4^{2-}}$ is also considerable.

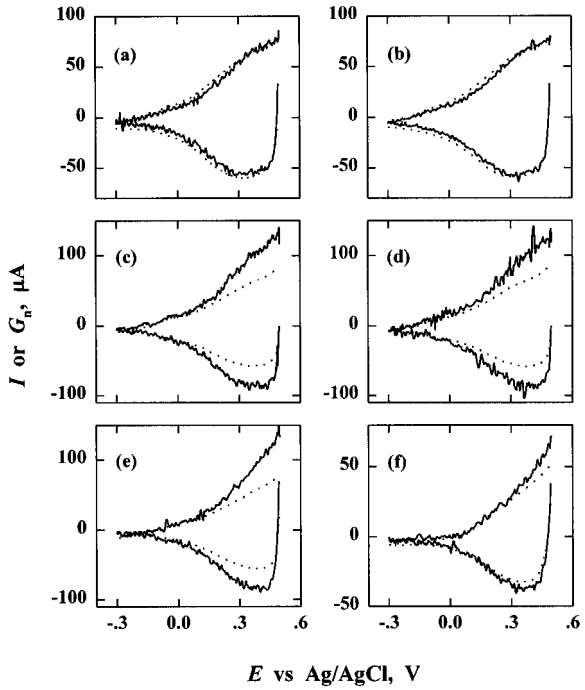

Figure 1. Cyclic voltammograms (I vs E, ···) and normalized mass change rate diagrams ($G_n = -(zF/W')G$ vs E, —) (scan rate = 10 mV/s) for PMPy/NO_3 films in (a) 0.1 M $Mg(NO_3)_2$ ($W' = W_{NO_3^-} = 62.0$) and (b) 0.1 M $Ba(NO_3)_2$ ($W' = W_{NO_3^-}$); for PMPy/Cl films in (c) 1 M $Mg(Cl)_2$ ($W' = W_{Cl^-} = 35.5$), (d) 1 M $Ba(Cl)_2$ ($W' = W_{Cl^-}$), and (e) 0.1 M $Mg(Cl)_2$ ($W' = W_{Cl^-}$); and for (f) PMPy/SO_4 in 1 M $MgSO_4$ ($W' = W_{SO_4^{2-}} = 96.0$).

In all cyclic EQCM experiments, as the redox cycle proceeds, total mass change (ΔM) and charge change (ΔQ) during the cathodic or anodic scan decrease gradually, but the ratio of ΔM to ΔQ is constant. It shows that the ion transport behavior and Y are uniform irrespective of the number of redox cycle. Even at the first cathodic scan, the ratio $\Delta M_c/\Delta Q_c$ is the same as that in the subsequent scan. It means that Y in the first cathodic scan is similar to that in the second one. It is known that the film after its deposition is compact. When a cation inserts into the compact film during the first cathodic scan, the break-in process occurs.[7a] But, when an anion excludes from the film, there is no break-in process. It was shown that, in PPy/CuPTS films, the amount of water that moves with a cation during the first cathodic scan is much larger than that during the subsequent scan.[2] On the other hand, in this experiment, there is no difference in Y between the first cathodic scan and the second one. It also indicates that cation transport is negligible.

Figure 2 shows electrochemical capacitance plots and simultaneously acquired electrogravimetric capacitance plots in the same systems as those in Figure 1. The electrochemical capacitance plot is normalized by the factor $-(W'/zF)$, i.e.,

$$(\Delta Q/\Delta E)_n = -(W'/zF)(\Delta Q/\Delta E) \quad (3)$$

where W' is fitted by adjusting an electrochemical semicircle to an electrogravimetric one. The fitted W' values are shown in Table 1.

The normalized electrochemical semicircle for a PMPy/NO_3 film in a 0.1 M $Mg(NO_3)_2$ solution (Figure 2a) shows good

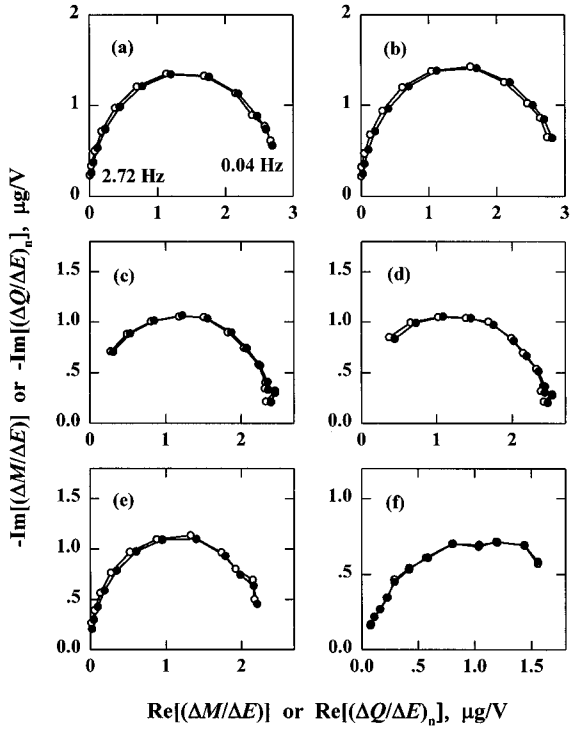

Figure 2. Electrogravimetric capacitance ($\Delta M/\Delta E$) (○) plots and normalized electrochemical capacitance ($(\Delta Q/\Delta E)_n = -(W'/zF)(\Delta Q/\Delta E)$) (●) plots at $E = 0.4$ V vs Ag/AgCl for PMPy/NO_3 films in (a) 0.1 M $Mg(NO_3)_2$ ($W' = 60$)) and (b) 0.1 M $Ba(NO_3)_2$ ($W' = 60$); for PMPy/Cl films in (c) 1 M $Mg(Cl)_2$ ($W' = 49$), (d) 1 M $Ba(Cl)_2$ ($W' = 49$), and (e) 0.1 M $Mg(Cl)_2$ ($W' = 49$); and for PMPy/SO_4 film in (f) 1 M $MgSO_4$ ($W' = 106$).

TABLE 1: Fitted W' and Y for PMPy Films in the Cyclic EQCM Experiment (Figure 1) and the Impedance Experiment (Figure 2)

		cyclic EQCM					
		cathodic		anodic		impedance	
polymer (solution)	E, V	W'	Y	W'	Y	W'	Y
PMPy/NO_3 (1 M $Mg(NO_3)_2$)	0.4	65	0.2	67	0.3	62	0.0
PMPy/NO_3 (0.1 M $Mg(NO_3)_2$)	0.4	63	0.1	67	0.3	60	
PMPy/NO_3 (0.1 M $Ba(NO_3)_2$)	0.4	62	0.0	65	0.2	60	
PMPy/Cl (1 M $Mg(Cl)_2$)	0.4	53	1.0	57	1.2	49	0.8
PMPy/Cl	0.3	52	0.9	54	1.0	47	0.6
(1 M $Ba(Cl)_2$)	0.4	53	1.0	55	1.1	49	0.8
	0.5					49	0.8
PMPy/Cl (0.1 M $Mg(Cl)_2$)	0.4	54	1.0	59	1.3	49	0.8
PMPy/SO_4 (1 M $MgSO_4$)	0.4	110	0.8	112	0.9	106	0.6
PMPy/SO_4 (0.1 M $MgSO_4$)	0.4	110	0.8	110	0.8	108	0.7

agreement with the electrogravimetric one, and the fitted W' (=60) is similar to $W_{NO_3^-}$ (=62.0). In a 0.1 M $Ba(NO_3)_2$ solution (Figure 2b), W' (=60) is the same as that in a 0.1 M $Mg(NO_3)_2$ solution. Similar to the cyclic EQCM experiment, all show that NO_3^- transport is dominant and that water transport is not large. For a PMPy/Cl film in a 1 M $Mg(Cl)_2$ solution (Figure 2c), the fitted W' (=49) is larger than W_{Cl^-} (=35.5). In a 1 M $Ba(Cl)_2$ solution (Figure 2d), W' (=49) is also larger than W_{Cl^-} (=35.5). The difference $W' - W_{Cl^-}$ corresponds approximately to the molar mass of 0.8 H_2O. It indicates that Cl^- moves with some waters into or out of the film. For a PMPy/SO_4 film in a 1 M $MgSO_4$ solution (Figure 2f), W' (=106)

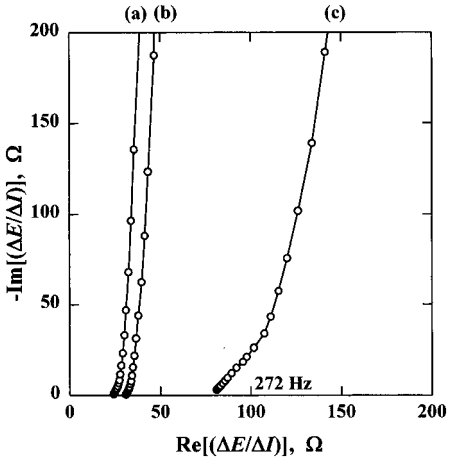

Figure 3. Electrochemical impedance ($\Delta E/\Delta I$) plots for (a) PMPy/NO_3 films in 1 M $Mg(NO_3)_2$ ($R_D = 47$), (b) PMPy/Cl films in 1 M $Mg(Cl)_2$ ($R_D = 43$), and (c) PMPy/SO_4 films in 1 M $MgSO_4$ ($R_D = 244$).

is also larger than $W_{SO_4^{2-}}$ (=96.0) and the difference $W' - W_{SO_4^{2-}}$ corresponds to the molar mass of 0.6 H_2O.

To compare mass transport in the cyclic EQCM experiment with that in the impedance experiment, W' in the cyclic EQCM experiment is fitted by adjusting G_n to I at the same potential as that in the impedance experiment. The fitted W' values are also shown in Table 1. The fitted W' during the cathodic scan is similar to that during the anodic scan. It means that Y is uniform at the same potential irrespective of scan direction. Every W' in the cyclic EQCM experiment is a little larger than that in the impedance experiment. For a PMPy/Cl film in a 1 M $Ba(Cl)_2$ solution, W' at 0.3 V during the cathodic or anodic scan is similar to that at 0.4 V (Table 1). And also, three W' values at 0.3, 0.4, and 0.5 V in the impedance experiment are similar. It seems that Y does not change extensively as the applied potential varies. On the other hand, it was shown that Y per cation exhibits the hysteresis behavior during the redox cycle and increases during insertion of a cation, whereas it is uniform during exclusion of a cation.[2]

In both cyclic experiment and impedance experiment, $Y_{NO_3^-}$ is smaller than Y_{Cl^-} and $Y_{SO_4^{2-}}$. The hydration enthalpy increases in order of NO_3^- (-309 kJ mol^{-1}) < Cl^- (-364 kJ mol^{-1}) < SO_4^{2-} (-1016 kJ mol^{-1}).[18] It was shown that the sequence of Y per alkali-metal ion in PPy/CuPTS films is the same as that of the hydration number of the ion.[2] Thus, Y per anion also relates to the hydration number of an anion. It was shown that Y per cation in PPy/CuPTS films increases as the concentration of an electrolyte solution decreases.[2] But, in this experiment, Y per anion does not depend on the concentration of an electrolyte solution. In a 0.1 M $Mg(Cl)_2$ solution (Figure 1e), I and G_n are similar to those in a 1 M $Mg(Cl)_2$ solution (Figure 1c). In a 0.1 M $Mg(Cl)_2$ solution (Figure 2f), W' (=49) is also similar to that in a 1 M $Mg(Cl)_2$ solution. In Table 1, every W' in a 1 M solution is similar to that in a corresponding 0.1 M solution.

Figure 3 shows electrochemical impedance plots for PMPy/NO_3, PMPy/Cl, and PMPy/SO_4 films. The ionic resistance in a film (R_D) is obtained by fitting the impedance data with the modified Randle's equivalent circuit.[19] It is interesting to note that R_D of a divalent anion SO_4^{2-} is much larger than those of monovalent anions. It means that the ionic conductivity of SO_4^{2-} in a film is much smaller than the ionic conductivities of NO_3^- and Cl^-. But, in an aqueous electrolyte solution, the difference in the ionic conductivity between SO_4^{2-} and NO_3^- or Cl^- is not large.[20] It was shown that the ionic conductivity

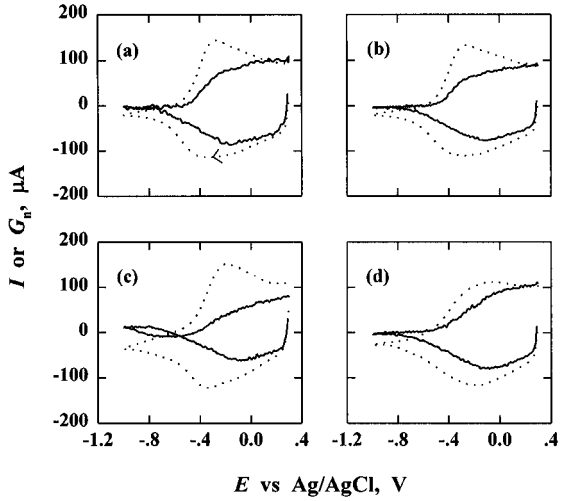

Figure 4. Cyclic voltammograms (I vs E, ···) and normalized mass change rate diagrams ($G_n = -(zF/W')G$ vs E, —) for PPy/NO_3 films (scan rate = 10 mV/s) in (a) 0.2 M $Ba(NO_3)_2$ ($W' = W_{NO_3^-} = 62.0$), (b) 0.2 M $Ca(NO_3)_2$ ($W' = W_{NO_3^-}$), (c) 0.2 M $Ba(NO_3)_2$ + 2 mM NaOH ($W' = W_{NO_3^-}$), and (d) 0.2 M $Ba(NO_3)_2$ + 0.01 M HNO_3 ($W' = W_{NO_3^-}$).

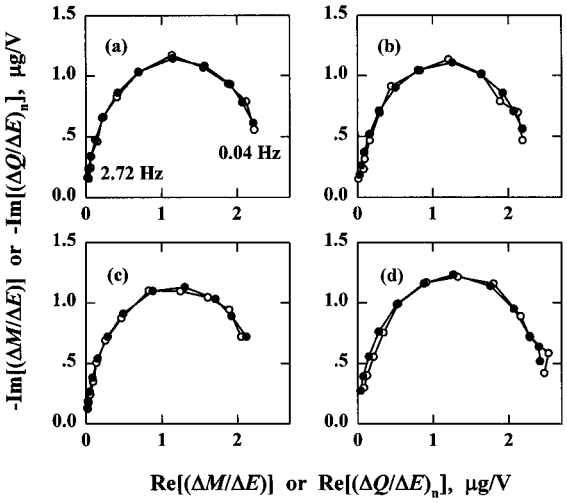

Figure 5. Electrogravimetric capacitance ($\Delta M/\Delta E$); (○) plots and normalized electrochemical capacitance ($(\Delta Q/\Delta E)_n = -(W'/zF)(\Delta Q/\Delta E)$) (●) plots for PPy/$NO_3$ films at $E = -0.1$ V vs Ag/AgCl in (a) 0.2 M $Ba(NO_3)_2$ ($W' = 31$), (b) 0.2 M $Ca(NO_3)_2$ ($W' = 31$), (c) 0.2 M $Ba(NO_3)_2/D_2O$ ($W' = 31$), and (d) 0.2 M $Ba(NO_3)_2$ + 0.01 M HNO_3 ($W' = 35$).

TABLE 2: Fitted W' for PPy/NO_3 Films at $E = -0.1$ V vs Ag/AgCl in the Cyclic EQCM Experiment (Figure 4) and the Impedance Experiment (Figure 5)

	cyclic EQCM		
solution	cathodic	anodic	impedance
0.2 M $Ba(NO_3)_2$	49	41	31
0.2 M $Ca(NO_3)_2$	47	40	31
0.2 M $Ba(NO_3)_2/D_2O$	49	40	31
0.2 M $Ba(NO_3)_2$ + 2 mM NaOH	38	21	
0.2 M $Ba(NO_3)_2$ + 0.01 M HNO_3	44	44	35

of a divalent cation is much smaller than that of a monovalent cation because of strong ion−ion interaction between the divalent ion and the charged polymer.[2] Likewise, it seems that the small ionic conductivity of SO_4^{2-} is due to strong ion−ion interaction in the film.

OH^- Transport in PPy/NO_3 and PPy/Cl Films. Cyclic voltammograms and mass change rate diagrams for PPy/NO_3 films are shown in Figure 4. Assuming NO_3^--specific ion transport ($W' = W_{NO_3^-}$), G is normalized by the factor $-(zF/W')$. Figure 5 shows electrogravimetric capacitance plots and electrochemical capacitance plots. The electrochemical capacitance plot is also normalized by the factor $-(W'/zF)$, where W' is fitted by adjusting an electrochemical semicircle to an electrogravimetric one. The fitted W' is shown in Table 2. Moreover, to compare mass transport in the cyclic EQCM experiment with that in the impedance experiment, W' in the cyclic EQCM experiment is fitted by adjusting G_n to I at the same potential as that in the impedance experiment. The fitted W' is also shown in Table 2.

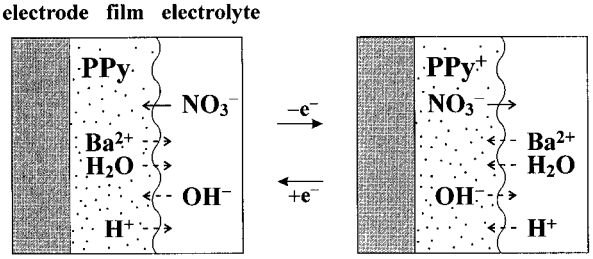

Figure 6. Possible four kinds of mass transport during the redox reaction of a PPy/NO_3 film in a $Ba(NO_3)_2$ solution.

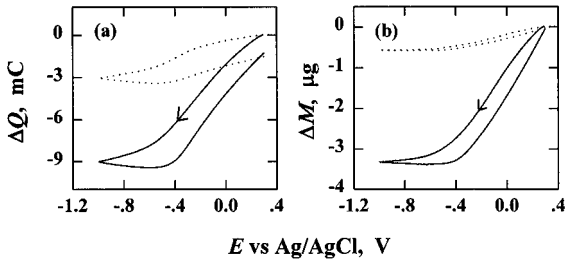

Figure 7. (a) Charge change diagrams (ΔQ vs E) and (b) mass change diagrams (ΔM vs E) for PPy/NO_3 films (scan rate = 10 mV/s, thickness = 0.2 μm (···) and 1 μm (—)) in 0.2 M $Ca(NO_3)_2$.

TABLE 3: ΔQ and ΔM during the Redox Cycle of PPy/NO_3 Films in 0.2 M $Ca(NO_3)_2$ (Figure 7)

thickness,	ΔQ, mC			ΔM, μg		
μm	ΔQ_c	ΔQ_a	$\lvert\Delta Q_c - \Delta Q_a\rvert$	ΔM_c	ΔM_a	$\lvert\Delta M_c - \Delta M_a\rvert$
0.2	−3.04	1.52	1.52	−0.57	0.54	0.03
1.0	−9.02	7.75	1.27	−3.32	3.27	0.05

In a 0.2 M $Ba(NO_3)_2$ solution (Figure 4a), G_n is much smaller than I in a wide potential range. Moreover, the fitted W' in the impedance experiment (Figure 5a) is 31, which is much smaller than $W_{NO_3^-}$ (=62.0). There are two possibilities for the small mass change. One is that faradaic processes that have nothing to do with the redox reaction of the film are present. The other is that another species in addition to NO_3^- participate in the mass change. Four kinds of transport are possible (Figure 6). The first is cation (Ba^{2+}) transport, and the second is water transport in the opposite direction of NO_3^- movement. The third and the last are the participation of OH^- and H^+, respectively, that exists in an aqueous solution.

Figure 7 shows ΔQ and ΔM during the redox cycle for PPy/NO_3 films in a 0.2 M $Ca(NO_3)_2$ solution. ΔQ_c and ΔM_c during the cathodic scan and ΔQ_a and ΔM_a during the anodic scan are shown in Table 3. The charge difference between $|\Delta Q_c|$ and $|\Delta Q_a|$ for the 0.2 and 1.0 μm thick films is 1.52 and 1.27 mC, respectively. The mass difference between $|\Delta M_c|$ and $|\Delta M_a|$ is 0.03 and 0.05 μg. Though the mass difference is small in comparison with $|\Delta M_c|$ and $|\Delta M_a|$, the charge difference is very large in comparison with $|\Delta Q_c|$ and $|\Delta Q_a|$. Moreover, the charge difference for the 0.2 μm thick film is similar to that for the 1.0 μm one. If the charge difference related to the redox reaction of the film, the charge difference for the 0.2 μm thick

film would be much smaller than that for the 1.0 μm one. It means that the charge difference is not due to the redox reaction of the film. $|\Delta Q_c|$ is always larger than $|\Delta Q_a|$ irrespective of the number of redox cycle, indicating that reduction processes unrelated to the reduction of the film are present. Because there is no electroactive species except the film and the aqueous solution, the reduction processes seem to relate to the reduction of the aqueous solution. To check this possibility, the solution pH is monitored for a thick PPy/NO_3 film (thickness = 10 μM) in a 0.2 M $Ca(NO_3)_2$ solution. The cell for pH measurement is composed of a double-compartment type connected by a glass frit. The pH value, which is measured after every 20th redox cycle, increases as 6.56, 7.34, 7.75, and 7.99. It means that the concentration of OH^- increases with the number of redox cycle. Thus, it is clear that the charge difference is due to the reduction of an aqueous solution. In Figure 4a,b, G_n at a more negative potential than −0.8 V is very small, indicating that the mass change of the film is nearly zero, but the reduction current is considerable. It shows that the reduction of an aqueous solution occurs largely in the low potential region. Consequently, the difference between I and G_n in the cyclic EQCM experiment is accounted for partly by the reduction of an aqueous solution.

In order to investigate the presence of cation transport, the responses in a Ba^{2+}-containing solution are compared with those in a Ca^{2+}-containing solution. G_n and I in Figure 4a show similar behavior with those in Figure 4b, and two fitted W' in capacitance plots of Figures 5a,b are also identical. If cation movement in the opposite direction of NO_3^- movement was considerable, G_n in a Ba^{2+}-containing solution would be smaller than that in a Ca^{2+}-containing solution because $W_{Ba^{2+}}$ (=137.3) is much larger than $W_{Ca^{2+}}$ (=40.1). It is evident that cation transport is negligible in this system.

If the difference between the fitted W' (=31) and $W_{NO_3^-}$ (=62.0) is associated with water movement in the opposite direction of NO_3^- movement, the difference ($W' - W_{NO_3^-}$ = 31) corresponds to the molar mass of 1.7 H_2O. Considering that the molar mass of 1.7 D_2O is 34, W' in a H_2O solution would be 3 larger than that in a D_2O solution. But two fitted W' in Figure 5a,c are identical, indicating that there is no opposite movement of water. Moreover, in the cyclic EQCM experiment, the fitted W' in a H_2O solution are similar to that in a D_2O solution (Table 2). Thus, the water movement opposite to NO_3^- movement can be excluded.

From experimental results, it is evident that cation or water movement opposite to NO_3^- movement is not present. Two possibilities, OH^- and H^+ transport, remains. It was reported that OH^- transport is involved during the redox reaction of PPy/NO_3 films and that dopant NO_3^- of PPy/NO_3 films is gradually replaced by OH^- after soaking in a neutral electrolyte solution.[8b,c] It was also reported that the contribution of H^+ transport is considerable during the redox reaction of PPy/Cl films that show similar behavior with PPy/NO_3 films in ion transport.[9] As the contribution of OH^- to ion transport increases, the mass change decreases because W_{OH^-} (=17.0) is much smaller than $W_{NO_3^-}$ (=62.0). If OH^- transport is present, the mass change in a more basic solution becomes smaller because of the increase in the contribution of OH^-. In a basic solution (Figure 4c), the mass change is smaller than those in Figure 4a,b. But, G_n at a more negative potential than −0.6 V is positive during the cathodic scan and is negative during the anodic scan. It means that the mass in this potential range increases during the cathodic scan and decreases during the anodic scan. It indicates that there is cation transport in a basic solution. Thus, it is impossible to know from the small mass change in a basic solution whether

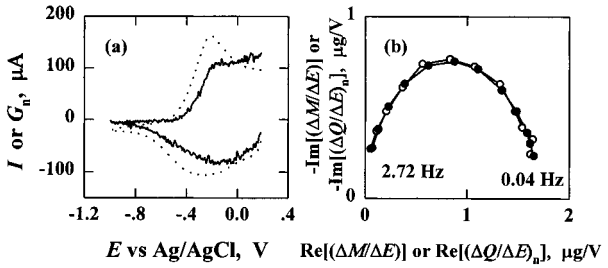

Figure 8. (a) A cyclic voltammogram (I vs E, ···) and a normalized mass change rate diagram ($G_n = -(zF/W')G$ vs E, —) (scan rate = 10 mV/s) ($W' = W_{Cl^-} = 35.5$) and (b) an electrogravimetric capacitance ($\Delta M/\Delta E$) (○) plot and a normalized electrochemical capacitance ($(\Delta Q/\Delta E)_n = -(W'/zF)(\Delta Q/\Delta E)$) (●) plot at $E = -0.1$ V vs Ag/AgCl ($W' = 25$) for a PPy/Cl film in 0.5 M $BaCl_2$.

OH^- transport is present or not, because cation transport also causes the decrease in the mass change. If the difference between the fitted W' (=31) and $W_{NO_3^-}$ (=62.0) is due to OH^- transport, W' in a D_2O solution is 0.7 larger than that in a D_2O solution because W_{OD^-} (=18) is large than W_{OH^-} (=17). But, because of experimental error and instrumental limit, it is impossible to confirm that small difference. In an acidic solution (Figure 4d), I and G_n differ from those in Figure 4a,b. The fitted W' in capacitance plots (Figure 5d) is 35, which is larger than those in Figure 5a−c. If H^+ transport was present, W' in more acidic solution would be smaller because of the increase in the contribution of H^+ to ion transport. It seems that the increase of W' in an acidic solution can be explained by the decrease in the contribution of OH^-. It is shown that OH^- is generated by the reduction of an aqueous solution during the redox cycle. Thus, the concentration of OH^- near a film is very high though it is not large in the bulk electrolyte solution. Probably, OH^- produced by the reduction of an aqueous solution takes part in ion transport. Consequently, it seems that OH^- transport in addition to NO_3^- occurs during the redox reaction of PPy/NO_3 films.

As the redox cycle proceeds, the mass transport behavior in a neutral solution changes gradually. It becomes different from that in Figure 4a,b, and becomes similar to that in a basic solution (Figure 4c). It is shown that the solution pH increases with the number of redox cycle and that cation in a basic solution takes part in ion transport. Thus, the mass transport behavior becomes complex as the redox cycle proceeds.

Figure 8a shows a cyclic voltammogram and a mass change rate diagram in a 0.5 M $BaCl_2$ solution for PPy/Cl films. Figure 8b shows an electrogravimetric capacitance plot and an electrochemical capacitance plot at −0.1 V. It shows that G_n in the cyclic EQCM experiment ($W' = W_{Cl^-}$) is smaller than I in most potential range. The fitted W' in the impedance experiment is 25, which is smaller than W_{Cl^-} (=35.5). It indicates that OH^- transport is important also during the redox reaction of PPy/Cl films.

It is shown that $Y_{NO_3^-}$ is not large in NO_3^--containing solutions for PMPy/NO_3 films and that Y_{Cl^-} is considerable in Cl^--containing solutions for PMPy/Cl films. But, it is difficult to measure Y in PPy/NO_3 and PPy/Cl films, because OH^- as well as NO_3^- or Cl^- transport take part in ion transport. G_n of Figure 4a,b is smaller than I in a overall potential range, whereas G_n of Figure 8a is larger than I at more positive potential than 0.0 V during the anodic scan. It seems that these behaviors are due to negligible $Y_{NO_3^-}$ and considerable Y_{Cl^-}.

Conclusions

Water transport behavior during anion transport was obtained from dynamic and steady-state behaviors of electrical and

gravimetric responses for PMPy/NO_3, PMPy/Cl, and PMPy/SO_4 films in electrolyte solutions containing a divalent cation. It is found that ion transport in these systems is anion-specific and that the number of accompanying waters per Cl^- or SO_4^{2-} is considerable, whereas the number per NO_3^- is not large. The number of accompanying waters per anion does not change extensively with the applied potential and the concentration of an electrolyte solution. Moreover, it is uniform irrespective of the number of redox cycle. The ionic conductivity of SO_4^{2-} is much larger than the ionic conductivities of NO_3^- and Cl^- because of strong ion−ion interaction in the film.

In PPy/NO_3 films and PPy/Cl films, the mass change during their redox reaction is much smaller than that of anion-specific ion transport. It is due to the reduction of an aqueous solution and the OH^- transport in addition to NO_3^- or Cl^- transport. There is no cation or water movement opposite to NO_3^- or Cl^- movement. Moreover, the production of OH^- by the reduction of an aqueous solution makes the mass transport behavior complex as the redox cycle proceeds.

Acknowledgment. This work was supported by the Korea Science and Engineering Foundation (Grant 94-0800-07-01-3).

References and Notes

(1) (a) Inzelt, G. In *Electroanalytical Chemistry*; Bard, A. J., Ed.; Marcel Dekker: New York, 1994; Vol. 18, p 89. (b) Lyons, M. E. G., In *Electroactive Polymer Electrochemistry*; Lyons, M. E. G., Ed.; Plenum: New York, 1994; Part 1, p 1.

(2) Yang, H.; Kwak, J. *J. Phys. Chem. B* **1997**, *101*, 774.

(3) Reynolds, J. R.; Pyo, M.; Qiu, Y.-J. *J. Electrochem. Soc*. **1994**, *141*, 35.

(4) (a) Buttry, D. A.; Ward, M. D. *Chem. Rev.* **1992**, *92*, 1355. (b) Buttry, D. A. In *Electroanalytical Chemistry*; Bard, A. J., Ed.; Marcel Dekker: New York, 1991; Vol. 17, p 1.

(5) (a) Southampton Electrochemistry Group. *Instrumental Methods in Electrochemistry*; Horwood: New York, 1993; Chapter 8. (b) Macdonald, J. R. *Impedance Spectroscopy*; Wiley: New York, 1987. (c) Musiani, M. M. *Electrochim. Acta* **1990**, *35*, 1665.

(6) (a) Bourkane, S.; Gabrielli, C.; Keddam, M. *J. Electroanal. Chem*. **1988**, *256*, 471. (b) Gabrielli, C.; Tribollet, B. *J. Electrochem. Soc*. **1994**, *141*, 1147.

(7) (a) Pei, Q.; Inganäs, O. *J. Phy. Chem*. **1993**, *97*, 6034. (b) Naoi, K.; Lien, M.; Smyrl, W. H. *J. Electrochem. Soc*. **1991**, *138*, 440.

(8) (a) Maia, G.; Torresi, R. M.; Ticianelli, E. A.; Nart, F. C. *J. Phys. Chem*. **1996**, *100*, 15910. (b) Li, Y.; Qian, R. *Synth. Met*. **1989**, *28*, C127. (c) Li, Y.; Qian, R. *J. Electroanal. Chem*. **1993**, *362*, 267.

(9) Bose, C. S. C.; Basak, S.; Rajeshwar, K. *J. Phys. Chem*. **1992**, *96*, 9899.

(10) Ren, X.; Pickup, P. G. *J. Phys. Chem*. **1993**, *97*, 5356.

(11) John, R.; Wallace, G. G. *J. Electroanal. Chem*. **1993**, *354*, 145.

(12) Pyo, M.; Reynolds, J. R. *J. Phys. Chem*. **1995**, *99*, 8249.

(13) (a) Inzelt, G.; Bácskai, J. *Electrochim. Acta* **1992**, *37*, 647. (b) Varineau, P. T.; Buttry, D. A. *J. Phys. Chem*. **1987**, *91*, 1292.

(14) Kelly, A. J.; Oyama, N. *J. Phys. Chem*. **1991**, *95*, 9579.

(15) (a) Ouyang, J.; Li, Y. *J. Appl. Polym. Sci*. **1996**, *61*, 1487. (b) Schmidt, V. M.; Heitbaum, J. *Electrochim. Acta* **1994**, *98*, 4861.

(16) Amemiya, T.; Hashimoto, K.; Fujishima, A. *J. Phys. Chem*. **1993**, *97*, 4187.

(17) (a) Martin, S. J.; Granstaff, V. E.; Frye, G. C. *Anal. Chem*. **1991**, *63*, 2272. (b) Yang, M.; Thompson, M. *Anal. Chem*. **1993**, *65*, 1158. (c) Noël, M. A. M.; Topart, P. A. *Anal. Chem*. **1994**, *66*, 484. (d) Topart, P. A.; Noël, M. A. M. *Anal. Chem*. **1994**, *66*, 2926. (e) Topart, P. A.; Noël, M. A. M.; Liess, H.-D. *Thin Solid Films* **1994**, *239*, 196.

(18) Erdey-Grúz, T. *Transport Phenomena in Aqueous Solutions*; Wiley: New York, 1974.

(19) (a) Duffitt, G. L.; Pickup, P. G. *J. Chem. Soc., Faraday Trans*. **1992**, *88*, 1417. (b) Rubinstein, I.; Sabatati, E.; Rishpon, J. *J. Electrochem. Soc*. **1987**, *134*, 3078. (c) Albery, W. J.; Elliott, C. M.; Mount, A. R. *J. Electroanal. Chem*. **1990**, *288*, 15.

(20) Atkins, P. W. *Physical Chemistry*, 4th ed.; Oxford University Press: Oxford, 1990.